Electronic structure and energetics of $B_xC_yN_z$ layered structures

Mário S. C. Mazzoni,[1] R. W. Nunes,[1,*] Sérgio Azevedo,[1,2] and H. Chacham[1,†]
[1]*Departamento de Física, ICEX, Universidade Federal de Minas Gerais, CP 702, 30123-970, Belo Horizonte, MG, Brazil*
[2]*Departamento de Física, Universidade Estadual de Feira de Santana, Km 3 BR-116, 44031-460, Feira de Santana, BA, Brazil*
(Received 23 November 2005; revised manuscript received 10 January 2006; published 27 February 2006)

We investigate the relative stability and electronic structure of several $B_xC_yN_z$ layered structures using first-principles calculations. The twenty structures we considered are derived from a graphite layer by placing carbon, nitrogen, or boron atoms on each site. Interestingly, a structure with $B_3C_2N_3$ stoichiometry was found to be more stable than the eight BC_2N structures in our study. The BCN compositions we considered present a wide range of electronic behaviors. In general, we observe that structures with large values of the electronic band gap have a B/N (x/z) ratio of one.

DOI: 10.1103/PhysRevB.73.073108 PACS number(s): 71.20.Tx, 71.15.Mb

Layered materials with sp^2 covalent bonding present a wide range of electronic and structural properties. Carbon nanotubes,[1] for instance, can be either semiconducting or metallic depending on their geometry,[2] while bulk graphite behaves as a semi-metal. Fully replacing carbon in graphite layers by alternating boron and nitrogen atoms leads to the formation of hexagonal boron nitride (h-BN), and to the opening of a large band gap which remains essentially unaltered when an h-BN sheet is rolled up to form a BN nanotube.[3] An interesting possibility is the partial substitution of carbon by boron and nitrogen in graphite, leading to the formation of ternary $B_xC_yN_z$ layered compounds of distinct stoichiometries, some of which have already been synthesized in chemical vapor deposition experiments.[4,5] This provides a route to the production of layered structures having electronic properties that are intermediate between those of graphite and h-BN, making it possible to tune the compound electronic structure to the needs of particular applications.

While some experimental works[6] have shown that BC_2N thin films emit visible light, even with indirect bandgaps,[7] similar experiments on $B_xC_yN_z$ nanotubes[8] indicate that transport properties depend on the relative C and BN fractions. Concerning structural properties of $B_xC_yN_z$ nanotubes and thin films, some synthesis methods lead to partial segregation between C and BN, which results in island-like configurations,[9] while others lead to structures in which C, B, and N atoms are mixed.[8,10] Previous first principles theoretical works have analyzed the electronic structure[11–13] and energetics[11] of a few specific BC_2N structures.

In this paper, we apply density-functional-theory (DFT) first-principles calculations to study the relative stability and electronic structure of $B_xC_yN_z$ layered structures with distinct atomic configurations and compositions. Our *ab initio* methodology is based on the density functional theory[14] as implemented in the SIESTA program.[15] We use norm-conserving Troullier-Martins pseudopotentials[16] in the Kleinman-Bylander factorized form,[17] and a double-ζ basis set composed of numerical atomic orbitals of finite range. Polarization orbitals are included for all atoms, and we make use of the generalized gradient approximation (GGA)[18] for the exchange-correlation potential. All geometries were relaxed until the total force on each atom was less than 0.05 eV/Å. We consider twenty distinct $B_xC_yN_z$ layered structures, with the unit cells indicated in Fig. 1. Four different stoichiometries are considered, namely, BCN_2, B_2CN, BC_2N, and $B_3C_2N_3$, as indicated in Table I.

In order to address the relative stability of the various $B_xC_yN_z$ structures under different stoichiometric conditions,[19] we introduce the theoretically calculated chemical potentials μ_N, μ_B, and μ_C for nitrogen, boron, and carbon, respectively. The chemical potentials for B and N are linked by the equilibrium thermodynamic condition $\mu_N + \mu_B = \mu_{BN}$, where $\mu_{BN} = -350.18$ eV is the chemical potential for a BN pair in bulk h-BN. Moreover, μ_N and μ_B may not exceed the chemical potential of the bulk phases, i.e., $\mu_{N(B)} \leqslant \mu^{bulk}_{N(B)}$. Under boron-rich conditions, the excess of B precipitates as bulk boron, hence we define our boron-rich environment by the limiting case $\mu_B = \mu^{bulk}_B$, where $\mu^{bulk}_B = -77.23$ eV is the total energy per atom for the metallic α-boron phase. From μ_B and the equilibrium constraint, we obtain $\mu_N = \mu_{BN} - \mu_B$. Similarly, in a nitrogen-rich environment we use $\mu_N = \mu^{bulk}_N$, where $\mu^{bulk}_N = -270.15$ eV is the total energy per atom of the $\alpha - N_2$ phase of solid nitrogen, and $\mu_B = \mu_{BN} - \mu_N$. The chemical potential for C, $\mu_C = 154.86$ eV, is obtained from a calculation for bulk graphene.

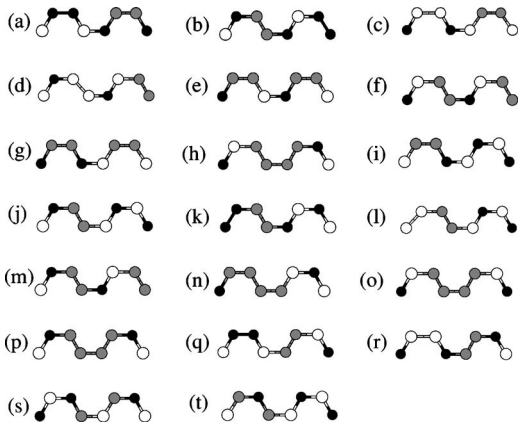

FIG. 1. $B_xC_yN_z$ layered structures considered in this work. Boron, carbon, and nitrogen atoms are represented by white, gray, and black circles, respectively.

TABLE I. Formation energies (in eV/atom) of the $B_xC_yN_z$ structures shown in Fig. 1, for N-rich (first column) and B-rich (second column) environments. In each case, the corresponding panel in Fig. 1 is indicated, and the band-gap energy (at the GGA level) is given in the last column.

Structure		N-Rich (eV/atom)	B-Rich (eV/atom)	E_{gap} (eV)
BCN_2	(a)	0.25	0.95	0.76
BCN_2	(b)	0.37	1.07	0.00
BCN_2	(k)	0.40	1.10	0.25
B_2CN	(c)	1.00	0.32	0.00
B_2CN	(d)	0.99	0.31	0.00
B_2CN	(l)	0.98	0.30	0.00
B_2CN	(e)	0.53	0.53	1.98
BC_2N	(f)	0.22	0.22	1.57
BC_2N	(g)	0.69	0.69	0.00
BC_2N	(h)	0.14	0.14	1.07
BC_2N	(m)	0.29	0.29	0.00
BC_2N	(n)	0.33	0.33	1.29
BC_2N	(o)	0.38	0.38	0.00
BC_2N	(p)	0.35	0.35	0.00
$B_3C_2N_3$	(i)	0.28	0.28	2.45
$B_3C_2N_3$	(j)	0.12	0.12	1.69
$B_3C_2N_3$	(q)	0.40	0.40	0.00
$B_3C_2N_3$	(r)	0.36	0.36	0.00
$B_3C_2N_3$	(s)	0.43	0.43	1.50
$B_3C_2N_3$	(t)	0.43	0.43	1.45

Using these chemical potentials, the formation energies of the structures are given by

$$E_f = E_{tot} - n_B\mu_B - n_N\mu_N - n_C\mu_C; \quad (1)$$

where E_{tot} is the total energy of the $B_xC_yN_z$ layer obtained from the supercell calculation, and n_B, n_N, and n_C are the number of B, N, and C atoms, respectively.

The results are shown in Table I for both boron- and nitrogen-rich environments. The $B_3C_2N_3$ structure in Fig. 1(j), showing a sequence of zig-zag C-C bonds, is found to be the most stable. Among the carbon-rich BC_2N structures, the most stable is the one shown in Fig. 1(h), which has the maximum number of C-C and B-N bonds, in a configuration that is suggestive of a segregated island-like structure. Its formation energy per atom is only slightly larger that that of the $B_3C_2N_3$ compound in Fig. 1(j).

Further, from Table I we can draw some general observations relating bonding patterns and stability of the BC_2N layers: Those with a zig-zag of C-C bonds [(f), (h), and (m)–(p)] have consistently lower energies than structures with a parallel sequence of C-C bonds, such as (e) and (g). While this trend is expected, since more C-C and B-N bonds are found in the zig-zag structures, it remains true even for structures such as (o) and (p), that contain one "wrong" B-B or N-N bond per unit cell, respectively. The enhanced stability of the carbon zig-zag chain compensates for the highly energetic B-B or N-N bond. Note also that between the structures (m) and (n) that have the same bond counting, structure (m), having all of its C-C bonds in a zig-zag pattern, has a slightly lower energy than structure (n), that contains a mixture of zig-zag and parallel C-C bonds.

The energetics of $B_3C_2N_3$ layers also points to a marked stability of zig-zag chains of C-C bonds, as indicated by a comparison of structures (i), (j), and (q)–(t). In particular, structures (q) and (r), containing one wrong bond per unit cell, have lower formation energies than structures (s) and (t), where no wrong bounds are found. Furthermore, these two latter structures are fully mixed, i.e., free of C-C bonds, and have much higher energies than structure (j). For the other stoichiometries, namely BCN_2 and B_2CN, the general trend is that nitrogen(boron)-rich structures are more stable in N(B)-rich environments, but with formation energies which are at least ~0.1 eV higher than the corresponding values for the most stable $B_3C_2N_3$ and BC_2N layered structures.

Overall, we can conclude that, in thermodynamical equilibrium, zig-zag arrangements of C-C bonds, as well as patterns with segregated h-BN and graphite islands, should be favored in $B_xC_yN_z$ layered structures. These results are in agreement with those of Blase *et al.* for BC_2N layers.[11] The tendency of formation of pure C and BN islands or stripes indicates that "correct" C-C and B-N bonds are favored over "wrong" C-N, C-B, B-B, and N-N bonds in $B_xC_yN_z$ layered structures. To quantify that effect in a simple way, we introduce a first-neighbor valence-bond model, based on a bond-energy parameterization of our *ab initio* results from the previous sections. The relevant parameters in the model are all possible first-neighbor bond energies, namely, ϵ_{CC}, ϵ_{CB}, ϵ_{CN}, ϵ_{NN}, ϵ_{BB}, and ϵ_{BN}. In terms of these quantities, the total energy in the model is given by

$$E^i_{tot} = \sum_{\alpha,\beta} n^i_{\alpha\beta}\epsilon^i_{\alpha\beta}, \quad (2)$$

where i is the structure index, α,β=C,B,N, and $n^i_{\alpha\beta}$ is the number of $\alpha\beta$ bonds in structure i. The parameters ϵ_{CC} and ϵ_{BN} are obtained from the calculations of the graphene and h-BN, respectively, and their values are ϵ_{CC}=−103.24 eV and ϵ_{BN}=−116.73 eV. The remaining parameters (ϵ_{CN}=−141.67 eV, ϵ_{NN}=−178.49 eV ϵ_{BB}=−50.40 eV, and ϵ_{CB}=−77.09 eV) are obtained by least-square fitting Eq. (2) to the *ab initio* total energies of the first ten $B_xC_yN_z$ structures in Figs. 1(a)–1(j). Although the model does not include explicitly effects of bond distortion and relaxation,[20] it does so implicitly, in an average way, through the optimized structures used in the fitting procedure.

In Fig. 2 we compare the *ab initio* results for the formation energies with those of the bond-energy model. The model formation energies E_f are calculated with Eqs. (1) and (2), using the chemical potentials calculated from first principles. The model gives results in good agreement with the *ab initio* ones (within 0.1 eV/atom) both for the structures used in the fitting (left panel of Fig. 2) and for those not used in the fitting (right panel of Fig. 2). The model can be used to shed some light on the stability trends previously reported. For instance, the model predicts that the energy cost to re-

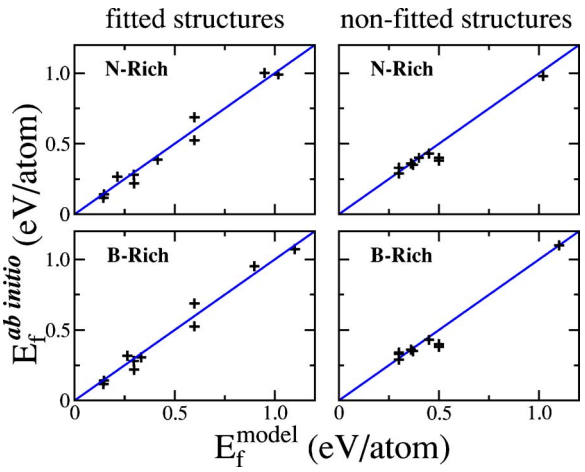

FIG. 2. (Color online) Formation energies per atom (in eV/atom) of the structures in Fig. 1, calculated using the bond-energy model of Eq. (2), vs the corresponding *ab initio* results.

place a pair of B-N and C-C bonds by a pair of B-C and N-C bonds is $\Delta\epsilon=(\epsilon_{CN}+\epsilon_{CB})-(\epsilon_{BN}+\epsilon_{CC})=1.21$ eV. This is consistent with the tendency of segregation into islands and stripes. The model also shows that formation of so-called wrong B-B and N-N bonds involves a high energy cost: An energy increase of $\Delta\epsilon=(\epsilon_{NN}+\epsilon_{BB})-2\times\epsilon_{BN}=4.57$ eV is associated with replacing a pair of B-N bonds by an N-N and a B-B bond, within the model.

Let us now discuss possible correlations between band gap and stability for the twenty $B_xC_yN_z$ structures considered here. Figure 3 shows the DFT-GGA band gap E_g as a function of the formation energy E_f for each structure. We mention that, for these systems, the GGA bandgaps should underestimate quasiparticle bandgaps by about 1.3 eV, from comparisons between our calculations and those of Blase *et al.*[11,21] Zero-gap structures that are metallic due to band overlap [Figs. 1(l), 1(q), and 1(r)] might become small-gap semiconductors upon a quasiparticle correction. On the other hand, the structures shown in Figs. 1(b)–1(d), 1(g), 1(m),

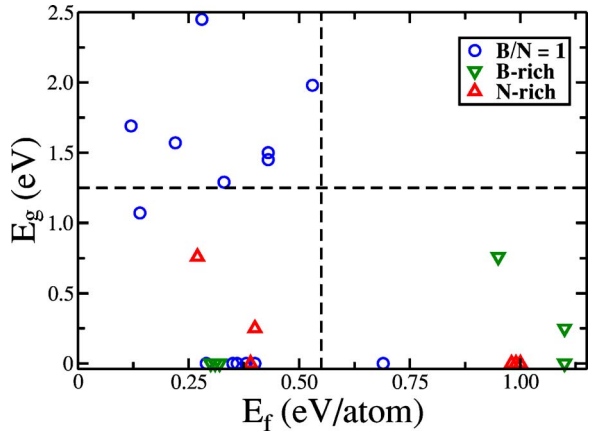

FIG. 3. (Color online) Electronic band gap E_g as a function of the formation energy E_f for the $B_xC_yN_z$ structures of Fig. 1. Structures with $x=z$ (B/N=1) are indicated by open circles. The remaining structures are indicated by open triangles, for N-rich and B-rich cases.

1(o), and 1(p) are metallic due to symmetry-related degeneracies and will not become insulating upon quasiparticle corrections. We also mention that the stacking of BN or BCN layers into "bulk" structures may considerably affect the bandgaps.[11,21] We observe that, generally, large band gaps are indicative of high stability, as suggested by the fact that no structure falls in the high-band-gap and high-formation-energy quadrant of Fig. 3, and by the marked tendency of the insulating structures to accumulate in the high-band-gap and low-formation-energy quadrant. Note, however, that the converse is not necessarily true: among the metallic structures, some have high values of E_f, while others show similar E_f values as the large band-gap ones. While these characterizations of "high" and "small" values for E_f and E_g are somewhat *ad hoc*, we believe that Fig. 3 should be indicative of general trends for $B_xC_yN_z$ layered structures.

Table I indicates that large band gaps are associated to stoichiometries with a B/N ratio of 1. On the other hand, six of the structures with B/N=1 are metallic. A more general trend is observed for the compositions with a B/N ratio different from 1, that have either small gaps or are metallic, with the exception of the BCN_2 compound in Fig. 1(a). Previous works[11,12] have analyzed the electronic structure of BC_2N layers on the basis of the symmetry representations of the electronic states of the pure graphene and BN layers. This, however, is only useful for compositions that retain some of the symmetry operations of the parent pure phases. Here, we adopt a local approach, by looking at the immediate neighborhood of the graphite-like zig-zag stripes or islands of C-C bonds. This allows us to identify certain composition patterns that lead to metallic (semi-metallic, in some cases) behavior.

Generally, an isolated zig-zag chain of carbon atoms displays metallic behavior whenever its immediate neighborhood is composed, on both sides, of atoms with an average valence not equal to four, regardless of the stoichiometry. This is the case for the BCN_2 [Fig. 1(b)] and B_2CN [Figs. 1(d) and 1(l)] structures that contain C-C zig-zag stripes surrounded on both sides by either nitrogen or boron. The same holds for the BC_2N structure (m), and also for the $B_3C_2N_3$ structures (q) and (r). The only exception is the BCN_2 structure (k), which has a small gap of 0.25 eV.

According to Blase *et al.*,[11] structures with neighboring C-C zig-zag stripes, forming phase-separated h-BN and graphite islands, have gaps that become progressively small as the lateral size of the graphite island increases. Here, we observe that, like in the case of isolated C-C zig-zag stripes, even the smaller island-like structures (o) and (p) might become metallic when surrounded on both sides by either boron or nitrogen atoms.

Due to the more delocalized nature of the boron valence orbitals, the zig-zag chain of boron atoms, present in structures (d) and (l), gives rise to a highly dispersive quasi-one-dimensional metallic band, along the chain direction. For the same reason, a chain of hexagonal B_2C_4 islands, such as in the structures (c) and (g), displays metallic behavior.

In summary, we have investigated the relative stability and electronic structure of several $B_xC_yN_z$ layered structures using first-principles calculations. Among the twenty structures we considered, the most stable has a $B_3C_2N_3$ stoichi-

ometry with lower formation energy than the eight BC_2N structures in our study. The structures present a wide range of electronic behaviors, with gaps varying from zero to 2.5 eV, at the DFT-GGA level. While we observe a correlation between large band gaps and stability, several metallic structures are found to have relatively low formation energies. In general, we observe that structures with large values for the electronic band gap have a B/N ratio of one. Moreover, we identify certain composition patterns that lead to the formation of metallic structures. Our results indicate that, in thermodynamical equilibrium, zig-zag arrangements of C-C bonds, and structures with phase-separated h-BN and graphite islands should be favored in $B_xC_yN_z$ layered structures. Finally, we propose a simple bond-energy model that reproduces quantitatively the first-principles results for the formation energies of the $B_xC_yN_z$ sheets.

We acknowledge support from the Brazilian agencies CNPq, FAPEMIG, and Instituto do Milênio em Nanociências-MCT.

*Electronic address: rwnunes@fisica.ufmg.br
†Electronic address: chacham@fisica.ufmg.br

[1] S. Iijima, Nature (London) **354**, 56 (1991).
[2] N. Hamada, S. I. Sawada, and A. Oshiyama, Phys. Rev. Lett. **68**, 1579 (1992).
[3] X. Blase, A. Rubio, S. G. Louie, and M. L. Cohen, Europhys. Lett. **28**, 335 (1994).
[4] A. R. Badzian, T. Niemyski, S. Appenheimer, and E. Olkusnik, in *Proceedings of the Intl. Conf. on Chemical Vapor Deposition*, edited by F. A. Glaski (American Nuclear Society, Hinsdale, IL, 1972), Vol. 3.
[5] J. Kouvetai, T. Sasaki, C. Shen, R. Hagiwara, M. Lerner, K. M. Krisnan, and N. Bartlett, Synth. Met. **34**, 1 (1989).
[6] M. O. Watanabe, S. Itoh, T. Sasaki, and K. Mizushima, Phys. Rev. Lett. **77**, 187 (1996); **77**, 2846 (1996).
[7] Y. Chen, J. C. Barnard, R. E. Palmer, M. O. Watanabe, and T. Sasaki, Phys. Rev. Lett. **83**, 2406 (1999).
[8] D. Golberg, P. Dorozhkin, Y. Bando, M. Hasegawa, and Z.-C. Dong, Chem. Phys. Lett. **359**, 220 (2002).
[9] Y. Zhang, K. Suenaga, C. Colliex, and S. Iijima, Science **281**, 973 (1998).
[10] M. O. Watanabe, S. Itoh, and K. Mizushima, Appl. Phys. Lett. **68**, 2962 (1996).
[11] X. Blase, J.-Ch. Charlier, A. De Vita, and R. Car, Appl. Phys. A **68**, 293 (1999); X. Blase, Comput. Mater. Sci. **17**, 107 (2000).
[12] A. Y. Liu, R. M. Wentzcovitch, and M. L. Cohen, Phys. Rev. B **39**, 1760 (1989).
[13] Y. Miyamoto, A. Rubio, M. L. Cohen, and S. G. Louie, Phys. Rev. B **50**, R4976 (1994); Y. Miyamoto, S. G. Louie, and M. L. Cohen, Phys. Rev. Lett. **76**, 2121 (1996).
[14] W. Kohn and J. Sham, Phys. Rev. **140**, A1133 (1965).
[15] D. Sanchez-Portal, P. Ordejon, E. Artacho, and J. M. Soler, Int. J. Quantum Chem. **65**, 453 (1997).
[16] N. Troullier and J. L. Martins, Phys. Rev. B **43**, 1993 (1991).
[17] L. Kleinman and D. M. Bylander, Phys. Rev. Lett. **48**, 1425 (1982).
[18] J. P. Perdew, K. Burke, and M. Ernzerhof, Phys. Rev. Lett. **77**, 3865 (1996).
[19] S. Azevedo, Mário S. C. Mazzoni, R. W. Nunes, and H. Chacham, Phys. Rev. B **70**, 205412 (2004).
[20] L. Wirtz, M. Lazzeri, F. Mauri, and A. Rubio, Phys. Rev. B **71**, 241402(R) (2005).
[21] X. Blase, A. Rubio, S. G. Louie, and M. L. Cohen, Phys. Rev. B **51**, 6868 (1995).